Pergamon

Int. J. Mach. Tools Manufact. Vol. 36, No. 7, pp. 799–816, 1996

0890–6955/96$15.00 + .00

0870–6955(95)00083-6

CHARACTERIZATION AND REAL-TIME MEASUREMENT OF GEOMETRICAL APPEARANCE OF THE WELD POOL

Y. M. ZHANG,† R. KOVACEVIC† and L. LI†

(*Received* 6 *April* 1995; *in final form* 24 *July* 1995)

Abstract—The weld pool contains important information about the welding process (Zhang *et al.*, *Welding J.* **72**, 463s–469s, 1993). In this study, a polar coordinate model is proposed to characterize the weld pool geometrically. The identification of its parameters involves complicated non-linear optimization which cannot be done in real time using conventional algorithms. A neural network is therefore proposed to identify the parameters in real time. By using pulsed laser illumination, clear images of the weld pool are captured. The developed image processing algorithm extracts the boundary of the weld pool in real time. Thus, a real-time system is developed to sense and process the image and identify the polar coordinate model. It is shown that the weld penetration can be accurately determined using the model parameters. Thus, a real-time weld penetration monitoring system is also achieved. Copyright © 1996 Elsevier Science Ltd

1. INTRODUCTION

During gas tungsten arc (GTA) welding, complicated phenomena occur on the surface of the weld pool [1]. Currently, it is nearly impossible to acquire all of the weld pool characteristics using a machine. Thus, only the major features of the weld pool should be of concern. To this end, extensive experimentation has been performed using GTA welding. It is shown that the geometry, i.e. the size and shape, of the weld pool contains sufficient information on the weld penetration. It is known that the weld penetration is a major determinant of the weld quality. Thus, the geometrical features of the weld pool should be sensed and controlled.

Assume that the boundary of the weld pool, represented by a set of boundary points, is available. It is evident that the geometrical features of the weld pool are completely contained in the set of boundary points. However, the features are not explicitly expressed. A parametric model must be proposed to characterize the weld pool. Its parameters must correspond to different characteristics of the weld pool. These parameters must be calculated based on the boundary points. Because these parameters will be controlled in the projected control system, the number of parameters should be kept to a minimum. To meet this requirement, a specific polar coordinate model is proposed. Using this model, the boundary of the weld pool can be described with sufficient accuracy.

In order to identify the model parameters, non-linear optimization will be required. If the conventional algorithms are used, the model will not be identified in real time. It has been shown that an artificial neural network is capable of modeling any type of non-linear relationship [2]. In fact, the capability associated with a neural network for approximating non-linear relationships can be increased by adding basic neurons [2]. The non-linear relationship can be approximated by adding neurons without knowing the actual architecture of the relationship, although the number of samples needed to train the network increases with the number of the neurons. In our case, numerous samples can be acquired. Thus, a neural network is adopted to correlate the model parameters with the boundary of the weld pool. Using the trained network, the parameters of the model can be identified in real time.

The model parameters of the weld pool have been measured from the trained network

†Welding Research and Development Laboratory Center for Robotics and Manufacturing Systems, University of Kentucky, Lexington, Kentucky, USA.

using the experimental records. It is shown that the weld penetration can be determined using the model parameters as accurately as when the full geometrical information of the weld pool is used.

2. EXPERIMENTATION

The experimental system is shown in Fig. 1. The welds are made using DCEN gas tungsten arc welding. The welding current is controlled in the range of 10–200 A by a computer through its analog output to the power supply. The torch and camera are attached to a three-axis computerized numerical controlled (CNC) position system. The motion can be preprogrammed and on-line modified by the computer in order to achieve the required torch speed and trajectory, including the arc length.

To calculate the parameters in the proposed model, an accurate boundary of the weld pool must be acquired. Although several approaches have been proposed to sense the geometry of the weld pool [3–7], vision sensing seems to be the most promising technique for obtaining a clear boundary of the weld pool. The difficulty in acquiring a clear boundary is the presence of the strong arc light. Coaxial viewing was proposed by Richardson *et al.*[8] and has been extensively investigated by a number of researchers. The idea is to block the arc light with the electrode when observing the weld pool. Also, since the weld pool surface is mirror-like, the diffuse reflection of the arc light from the weld pool surface is weaker than that from the solid surrounding area. But, due to the radiation from the weld pool, the intensity contrast of the pool surface against the surrounding area is low. Even though excellent algorithms have been developed, it still requires 6.5 seconds on a VAX 11/785 computer [9], or a few tens of seconds on a 12 MHz 80286-based machine [10], in order to extract the pool boundary from an ideal image, i.e. without oxides or impurities on the pool. To control the arc-welding process, it is desired that the feedback of the weld pool can be at least 2 Hz. Thus, a pulsed laser with a peak intensity that is much higher than the intensity of the arc light, was projected on to the weld pool and its surrounding area [11]. Because the weld pool surface is mirror-like, the projected laser is specularly reflected from the surface of the weld pool. The corresponding image of the weld pool is therefore dark. But from the solid area surrounding the weld pool, the projected laser is diffusely reflected. The resultant image is bright. Thus, the weld pool can be very clearly viewed. Based on this idea, a vision sensor has been developed by Control Vision, Inc. [11]. This sensor was used in a previous study, and a real-time image processing algorithm was developed to extract accurately the weld pool boundary in less than 200 ms, despite the variations in the surface and welding conditions [12]. Thus, the pool boundary

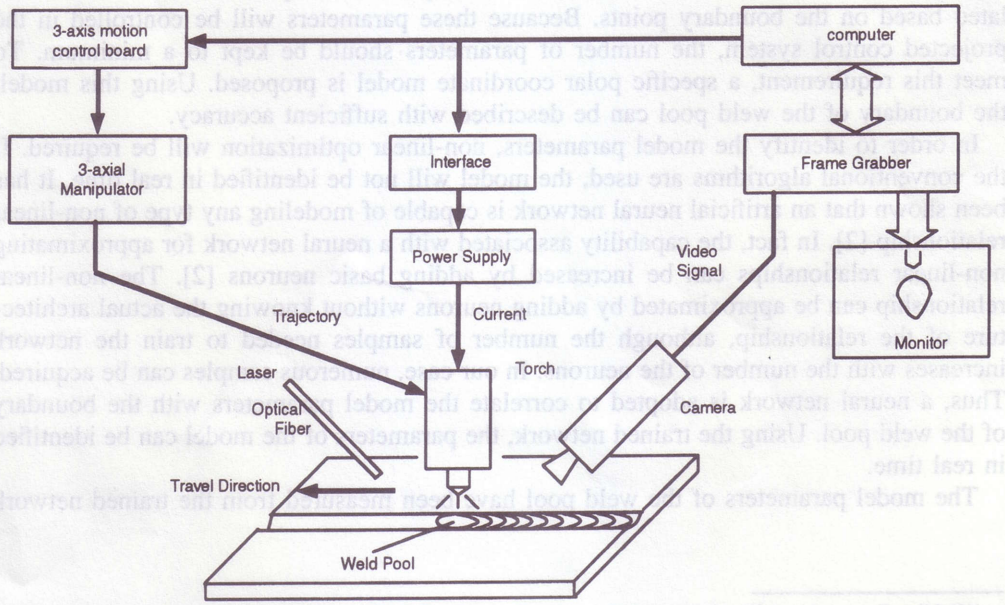

Fig. 1. Experimental set-up.

could be acquired to identify the parameters in the proposed model. In this study, this sensor will be used to acquire a clear image of the weld pool.

The camera views the weld pool region at a 45° angle from the rear of the weld pool. The frame grabber digitizes the video signal into a 512 × 512 8 bit digital image matrix. The pulse of the laser lasts only 3 ns. Although the average power of the laser is only 7 mW, its peak power reaches 70 kW. The acquired images are shown in Fig. 2.

Variations in weld pool can be generated by different welding parameters. These parameters include the welding current, arc length, travel speed, electrode tip angle, and rate of the shielding gas flow. In order to find a valid approach to characterize the weld pool, the major parameters which may vary during welding should be considered in the experiments. In this study, the material is stainless steel 304, with a thickness of 3 mm. Bead-on-plate and butt welds are made. The objective is to characterize the fully penetrated weld pool. Varied current, arc length

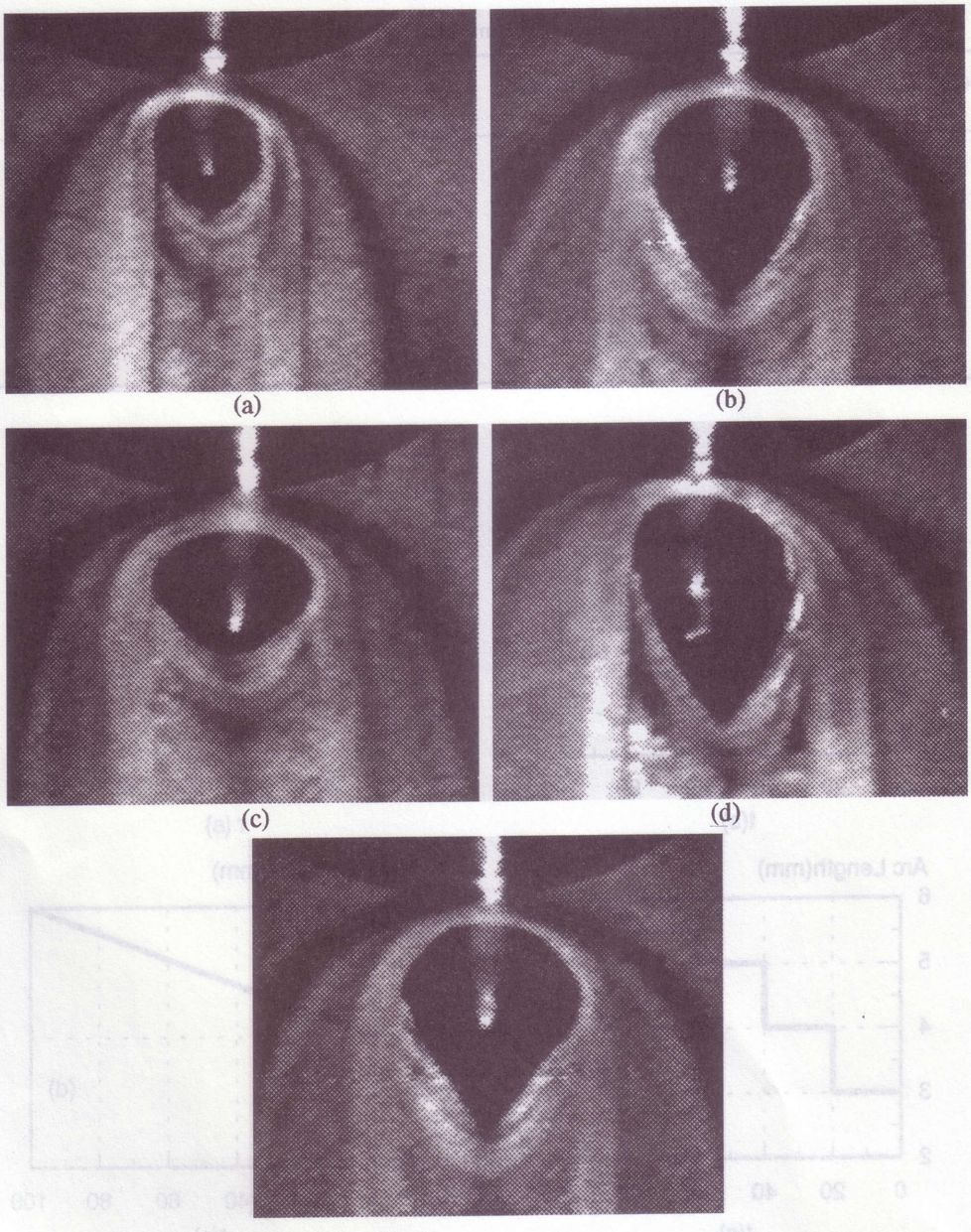

Fig. 2. Typical weld pools: (a) small pool; (b) large pool; (c) wide pool; (d) long pool; (e) sharp pool.

and travel speed are selected to make the weld pool geometry vary in the range of interest. The experimental conditions are detailed in Table 1 and Fig. 3.

3. MODELING OF THE WELD POOL BOUNDARY

The geometrical features of the weld pool are contained in the set of boundary points. Although the length L and relative widths w_r's (Fig. 4) can present a sufficient approximation to the geometrical features of the weld pool, the number of parameters may be too high to control using the prospective control system. If the number of the relative widths is reduced, the accuracy will be decreased as well. Thus, another characterization should be used. In this study, the boundary will be modeled. The objective is to describe the boundary of the weld pool with sufficient accuracy using fewer parameters.

Different approaches may be used to describe closed boundaries [13]. For a closed boundary such as the weld pool boundary in which each radius vector from the centroid of the boundary

Table 1. Experimental conditions

No.	Current (A)	Arc length (mm)	Speed (mm/s)	Gap	Ar flow rate (SCFH)
1	100	3	3	–	30
2	100	3	2.5	–	30
3	see Fig. 3(a)	3	2	–	30
4	100	3	2	–	25
5	100	3	2	–	30
6	100	see Fig. 3(b)	2	–	30
7	100	see Fig. 3(c)	2	–	30
8	100	3	1.5	–	35
9	100	3	1.5	see Fig. 3(d)	30

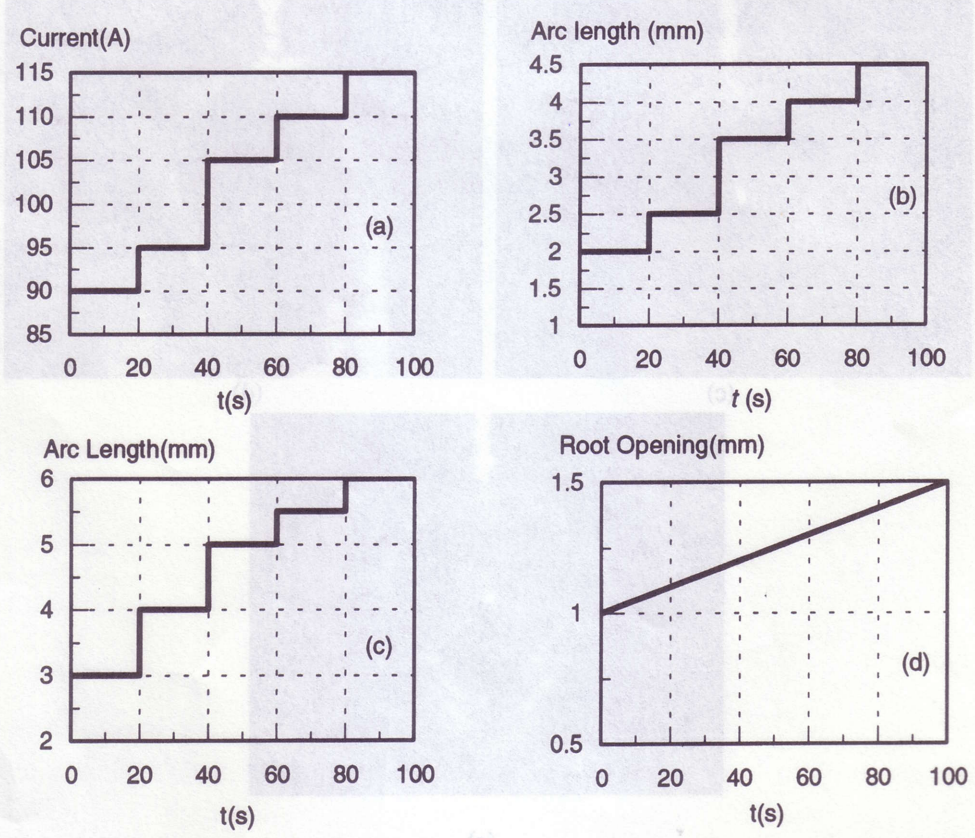

Fig. 3. Partial experimental parameters: (a) current variation in experiment 3; (b) arc length variation in experiment 6; (c) arc length variation in experiment 7; (d) root opening in experiment 9.

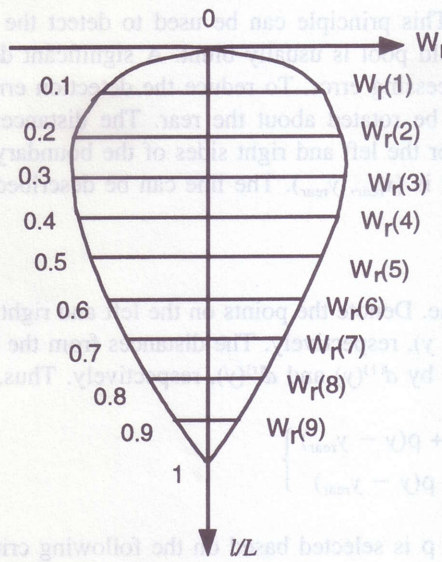

Fig. 4. Convectional description of the weld pool. If the number of the used relative widths is sufficient, the length and relative widths can provide a sufficient description of the geometry of the weld pool.

intersects the boundary at only one point, a one-dimensional series of real numbers can be acquired by measuring the lengths of successive radius vectors which are angularly equispaced. This series is denoted as $\{r(\alpha)\}$, where $r(\alpha)$ is the radius of the vector at the angle α. Thus, for a closed pool boundary, $\{r(\alpha)\}$ can be used to describe its shape.

The following polar coordinate model is used to describe the pool boundary in this study:

$$r(\alpha) = \theta_0 + \sum_{j=1}^{p} \theta_j \alpha^{\theta_{p+j}} \tag{1}$$

where $\theta = (\theta_0, \theta_1, ..., \theta_{p+1}, ..., \theta_{2p})^T$ is the parameter vector, and p is the order. It has been shown by modeling experimentation that it is very difficult to describe the pool boundary sufficiently, even using a high p. However, the pool boundary can be described with sufficient accuracy using a low p if the boundary is modeled piecewisely. Thus, the left and right boundaries can be modeled using equation (1), separately. In order to do this, the boundary must be segmented into left and right halves.

The rear and front points of the weld pool should be detected first. Since the torch travels along the negative x direction of the work coordinate system (Fig. 5), the points of the boundary which have the minimum and maximum x coordinates should be the front and rear points of

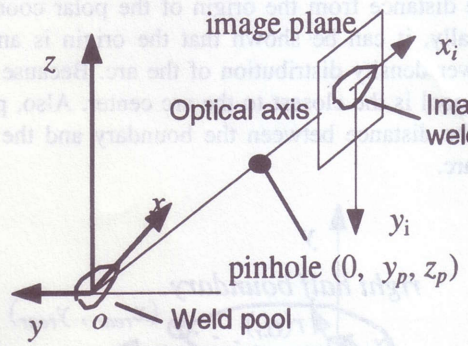

Fig. 5. The work and image coordinate systems. xyz is the work coordinate system attached to the workpiece. x_i y_i is the image coordinate system. The xy plane is the surface of the workpiece. The axis of the electrode is the z axis. The camera is attached to and moves with the torch. The torch moves along the negative x direction. The camera views the weld pool from the side, i.e. the x_i axis is parallel to the x axis and the optical axis of the camera crosses the origin, o, of the work coordinate system.

the weld pool, respectively. This principle can be used to detect the rear of the weld pool. However, the front of the weld pool is usually blunt. A significant detection error could be caused by a small image processing error. To reduce the detection error, a line can be made from the rear. This line can be rotated about the rear. The distances from this line to the boundary can be calculated for the left and right sides of the boundary, respectively. Assume that the rear of the weld pool is (x_{rear}, y_{rear}). The line can be described by:

$$x = x_{rear} + \rho(y - y_{rear}) \tag{2}$$

where ρ is the slope of the line. Denote the points on the left and right edges of the weld pool as $(x[(1)](y), y)$ and $(x[(r)](y), y)$, respectively. The distances from the left and right boundary points to the line are denoted by $d^{(1)}(y)$ and $d^{(r)}(y)$, respectively. Thus,

$$\left.\begin{aligned} d^{(1)}(y) &= -x^{(1)}(y) + x_{rear} + \rho(y - y_{rear}) \\ d^{(r)}(y) &= x^{(r)}(y) - x_{rear} - \rho(y - y_{rear}) \end{aligned}\right\} \tag{3}$$

To segment the weld pool, ρ is selected based on the following criterion:

$$\rho: \min_{\rho \in R^1} \sum_{y} (d^{(1)}(y) - d^{(r)}(y))^2 \tag{4}$$

where R^1 is a real number. It can be shown that the determination of ρ is a standard linear least squares problem and the solution can be acquired by applying the standard least squares algorithm [14]. The resultant line is used as the segment line to divide the boundary into the left and right halves. Using the segment line, the front point can also be obtained.

Ideally, the weld pool should be symmetric about the segment line. Thus, the angle α can be defined for the left and right halves, respectively, as shown in Fig. 6. Because of this definition, the models for the left and right halves will be the same in the ideal case. The parameters required for describing the boundary are therefore decreased.

The objective of modeling the boundary is to characterize the weld pool. To acquire an exact description of the weld pool, all points of the boundary must be used. But, as known, the characteristics of the weld pool are not explicitly expressed. It is clear that as few as possible parameters should be used in order to understand the roles of each parameter in describing the weld pool. Thus, the number of parameters should be small. As described above, by means of the angle definition, the boundary can be described by using a single model. The following model is proposed:

$$r(\alpha) = \theta_0 + \theta_1\alpha^2 + \theta_2\alpha^{\theta_3} \tag{5}$$

It is apparent that θ_0 is the distance from the origin of the polar coordinate system to the front of the weld pool. Actually, it can be shown that the origin is an estimate of the arc center. θ_0 depends on the power density distribution of the arc. Because of the movement of the arc, the front of the weld pool is the closest to the arc center. Also, progressing along the pool edge towards the rear, the distance between the boundary and the arc center increases due to the movement of the arc.

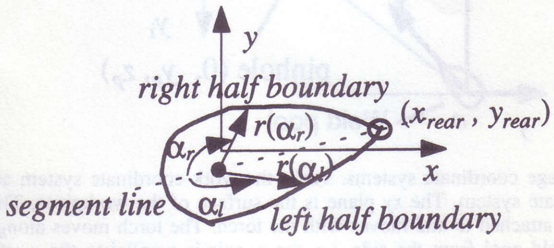

Fig. 6. Polar coordinate description of boundary.

θ_1 is a major parameter for describing the size of the weld pool. In Fig. 7(a), three boundaries with different θ_1 are plotted. (The other parameters are the same.) It can be seen that no significant change of the shape can be observed, but the size of both the width and length increases with θ_1. It is known that the length of the weld pool is much larger than the pool width. The greatest width occurs when $\alpha > \pi/2$. If α^1 is used instead of α^2, the ratio between the increases in the length and width of the weld pool will be too small to maintain the shape of the weld pool. When α^2 is used, this ratio can be increased to retain the shape of the weld pool.

An important feature of the weld pool is the sharpness of the pool rear. To explain the concept of sharpness, three weld pools are shown in Fig. 7(b). A sharper pool is generated with a larger θ_3. This sharpness feature cannot be described by θ_1 effectively. But θ_3 provides an effective description of this feature. In fact, as θ_3 increases, the rate of increase in distance from the arc center to the boundary increases.

Three different boundaries are illustrated in Fig. 7 (c). The parameters used to generate these boundaries are the same except for θ_2. It can be seen that the weld pool becomes more narrow when θ_2 increases. However, the sharpness of the rear does not significantly change. Consequently, θ_2 can be used to describe the narrowness of the weld pool.

The above analysis shows that different features of the weld pool can be described by the parameters of the polar coordinate model. Thus, the proposed polar coordinate model will be

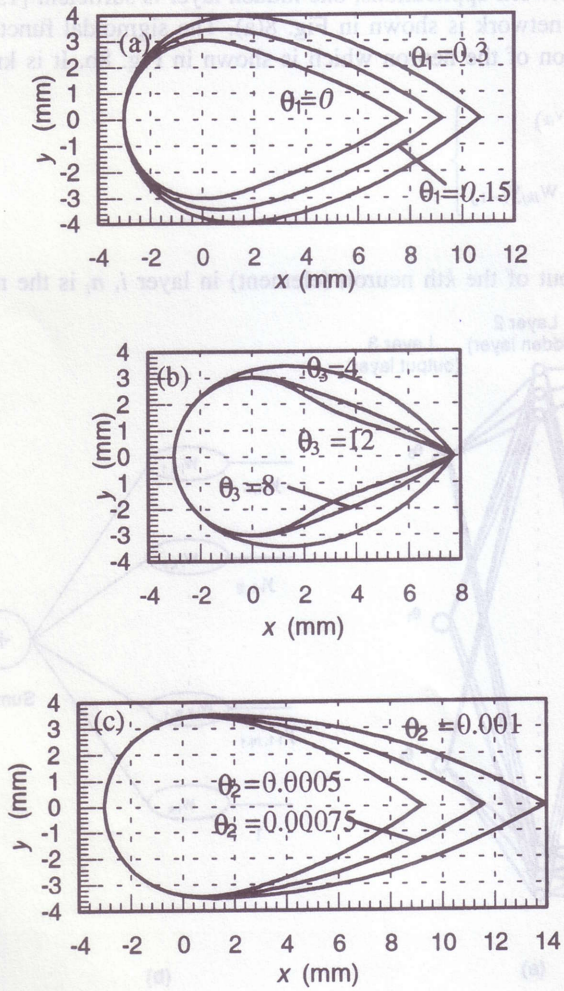

Fig. 7. Pool geometrical feature and modeling: (a) pool size change (θ_0 = 3.0 mm, θ_2 = 0.005 mm, θ_3 = 8); (b) sharpness change of pool rear (θ_0 = 3.0 mm, θ_1 = 0, θ_2 = 0.0005 π^4 mm for θ_3 = 4, θ_2 = 0.0005 mm for θ_3 = 8, θ_2 = 0.0005 mm/π^4 for θ_3 = 8); (c) narrowness change (θ_0 = 3.0 mm, θ_1 = 0.15 mm, θ_3 = 8).

used to model the geometrical features of the weld pool. Its parameters should be identified on-line for intelligent control.

4. REAL-TIME IDENTIFICATION

In order to acquire the model, the origin of the polar coordinate system, denoted as (x_0, y_0), must be carefully selected. The criterion for estimating the parameters in Eq. (5) is:

$$\hat{\theta}: \min_{\theta \in R^{2p+1}} \left\{ \sum_{j=1}^{N^{(l)}} (\sqrt{x^{(l)}(j) - x_0)^2 + (y^{(l)}(j) - y_0)^2} - r(\alpha(j))^2 \right. \\ \left. + \sum_{j=1}^{N^{(r)}} (\sqrt{x^{(r)}(j) - x_0)^2 + (y^{(r)}(j) - y_0)^2} - r(\alpha(j))^2 \right. \tag{6}$$

where $(x^{(l)}(j), y^{(l)}(j))$ $(j = 1,...,N^{(l)})$ and $x^{(r)}(j), y^{(r)}(j))$ $(j=1,...,N^{(r)})$ are the points of the left and right halves of the weld pool boundary, respectively, and $\alpha(j)$ is the angle corresponding to these points. It can be shown that $\alpha(j)$ is a function of both the boundary points and origin, (x_0, y_0), of the polar coordinate system. A complex non-linear function must be minimized with respect to the parameters of the polar coordinate model and (x_0, y_0). This will be difficult to complete on-line using the conventional optimization algorithms. In order to identify the model in real time, a neural network is used.

For most neural network applications, one hidden layer is sufficient [15]. Thus, the architecture of the resultant network is shown in Fig. 8(a). The sigmoidal function [2] is selected as the non-linear function of the neuron which is shown in Fig. 8b. It is known [2]:

$$\left. \begin{aligned} y_{i,k} &= 1/(1 + e^{-v_{ik}}) \\ v_{ik} &= w_{ik} + \sum_{j=1}^{n_{i-1}} w_{ikj} y_{i-1,j} \end{aligned} \right\} \tag{7}$$

where $y_{i,k}$ is the output of the kth neuron (element) in layer i, n_i is the number of neurons in

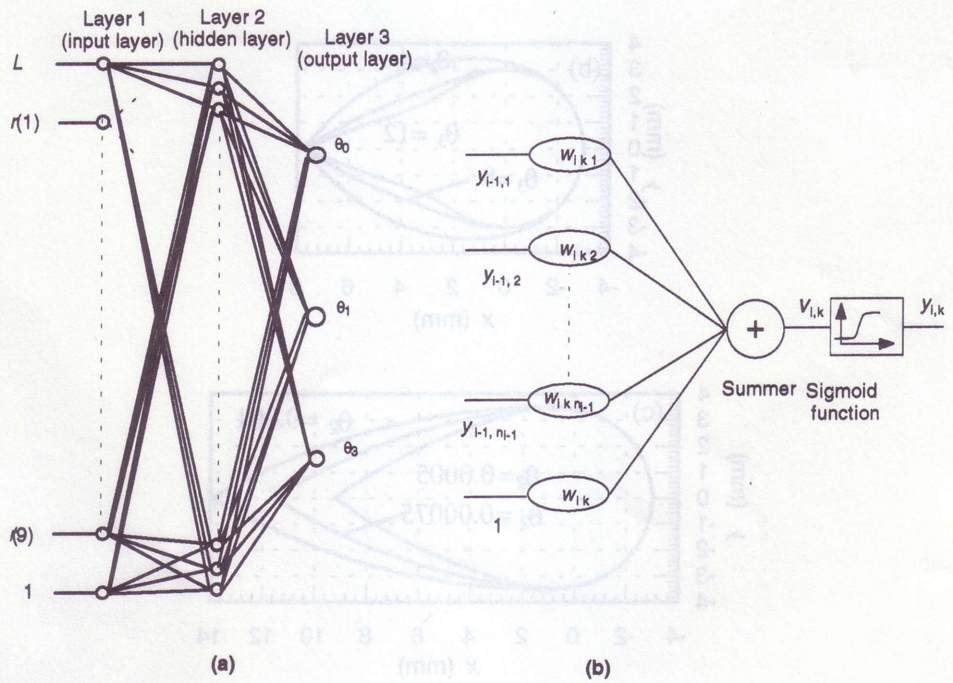

Fig. 8. Neural network model for identifying the polar coordinate model. $r(j)$ $(j = 1,...,9)$ are the relative widths and L is the length of the weld pool. The ouputs of the network are the parameters of the polar coordinate model. θ_2 can be calculated based on θ_j $(j = 0,1,3)$ and L: (a) architecture; (b) neuron structure.

layer i, and w_{ik} and w_{ikj} are the weights of the neuron which must be determined by the training process.

The number of elements in the hidden layer, denoted as n_2, can be selected by the following equation [15]:

$$n_2 = N/10(n_1 + n_3) \sim N/5(n_1 + n_3) \tag{8}$$

where N is the number of samples, and n_1 and n_3 are the number of elements in the input and output layer, respectively.

The data used to train the network can be calculated using the following steps:

(1) Assume that the possible range for the weld pool length is $L \in$ (7 mm, 20 mm).
(2) Assume that the possible range for θ_0 is $\theta_0 \in (L/10, L/3)$.
(3) For the given L and θ_0, the parameters of the model will have the restriction: $\theta_1\pi^2 + \theta_2\pi^{\theta_3} = L - 2\theta_0$. Using this restriction, possible θ_j (j = 1,2,3) can be used to calculate the radius of the vector. Thus, closed boundaries can be acquired.
(4) Each closed boundary is divided into 10 equidistant segments along the torch travel direction. Using the location of these segments, nine widths of the weld pool can be measured along the weld pool length. Dividing by the length of the weld pool gives the nine relative widths shown in Fig. 4.

The length and nine relative widths are used as the inputs of the network. The outputs of the network are the model parameters. It can be shown that only three of θ_j (j = 0,1,2,3) are independent when the length is known. Thus, θ_j's (j = 0,1,3) are selected as the outputs of the network. θ_2 can be calculated using the length and θ_j's (j = 0,1,3). The sigmoidal function is selected as the non-linear function of the neuron [2]. The number of samples used for network training is 8000. A single hidden layer was employed. It was shown that sufficient accuracy of the neural network modeling can be acquired with 20 elements in the hidden layer.

The training was performed using commercial neural network software. The algorithm is the extended delta-bar-delta (EDD) which can overcome the slow convergence associated with the conventional back-propagation algorithm. The learning ratio is automatically determined by the algorithm. The training cycle is selected to be 50,000. In Fig. 9, the training results are illustrated. It can be seen that θ_0 has been accurately traced, whereas errors can be observed for θ_1 and θ_3. The maximum errors in θ_1 and θ_3 are about 0.08 mm and 3, respectively. Because variation ranges of θ_1 and θ_3 are 0.5 mm and 14, the maximum relative errors are about 20%. However, it is found that the large errors in estimating θ_1 and θ_3 only occur when the θ_3 used is close to 2. In this case, the coupling between α^2 and α^{θ_3} exists. Thus, considering the accuracy in θ_0 and the $\theta_1\pi^2 + \theta_2\pi^{\theta_3} = L - 2\theta_0$ for calculating θ_2, the actual total modeling accuracy was accepted.

For the measured boundary of the pool, the rear and segment line (Fig. 6) are acquired first. Then the length is determined using the rear and front points. The nine widths are measured normal to the segment line. From these measurements, the parameters of the model are calculated from the neural network.

To identify the geometrical feature of the weld pool in real time, the developed neural network has been incorporated with the image sensor, image processing algorithm and welding machine. The image is processed using a real-time image processing algorithm developed in our previous study [12]. The acquired points of the boundary are transformed from the image coordinates into the work coordinates. Then the nine relative widths and length of the weld pool are calculated and used as the inputs for the neural network. The outputs of the network are the parameters of the polar coordinate model. Because of the real-time image processing and neural network, the model parameters can be calculated in 200 ms. Thus, the characteristics of the weld pool can be identified in real time.

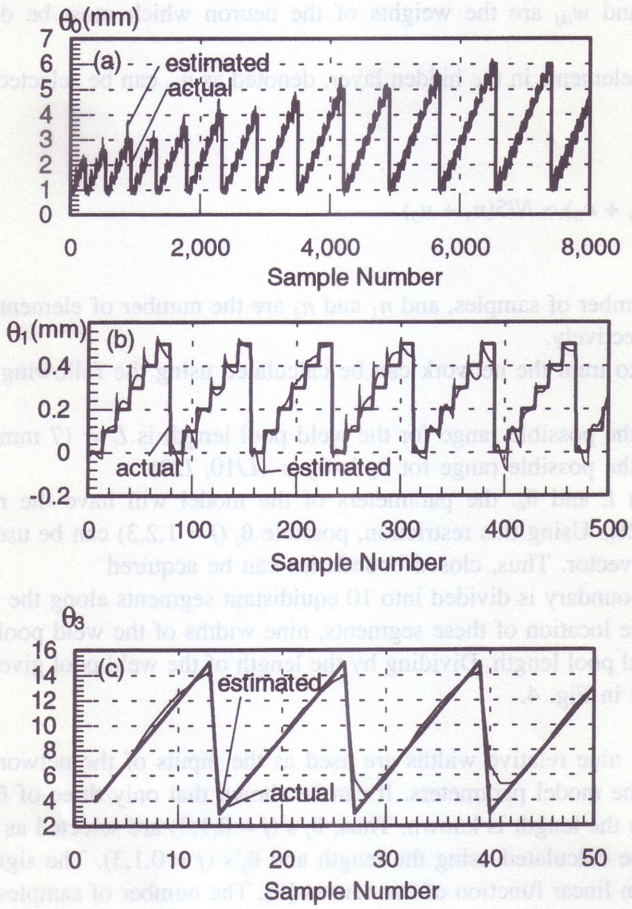

Fig. 9. Neuronal network estimates of polar coordinate model. The number of samples used to train the network is 8000. θ_1 and θ_3 vary very fast in its range. Also, the variation pattern is repeated. To show the variations in θ_1 and θ_3, only the first 500 and 50 data are plotted, respectively: (a) parameter θ_0; (b) parameter θ_1; (c) parameter θ_3.

5. RESULTS AND DISCUSSION

Sufficiency in characterizing weld pool

The boundaries shown in Fig. 10(a) are acquired from the images shown in Fig. 2 using the image processing algorithms [12] and coordinate transformation. These weld pools have different geometrical features. Using their length and relative widths, the parameters of the polar coordinate model have been acquired using the trained network. The resultant boundaries are shown in Fig. 10(b). It can be seen that the original geometrical features of the weld pools have been sufficiently described by the modeled boundaries.

It is known that the weld penetration is a major determinant of the weld quality. Extensive studies have been performed to find a feasible approach to sense and control the weld penetration [16–18]. In order to show the sufficiency of the proposed model in characterizing the weld quality, the weld penetration can be modeled using the full description of the weld pool, i.e. the length and nine relative widths, and the polar coordinate model parameters, respectively.

In Fig. 11, the measured length and width are plotted in addition to the measured back-side bead width which specifies the full penetration status [1]. Different weld pool parameters have been used as inputs for the neural network to calculate the back-side bead widths (Fig. 12). It can be seen that the back-side bead width can be calculated with satisfactory accuracy using the length and nine relative widths (Fig. 12a). However, the accuracy associated with each individual parameter is much poorer (Fig. 12b, c). When both the length and width are used, the resultant modeling accuracy improvement is not significant (Fig. 12d).

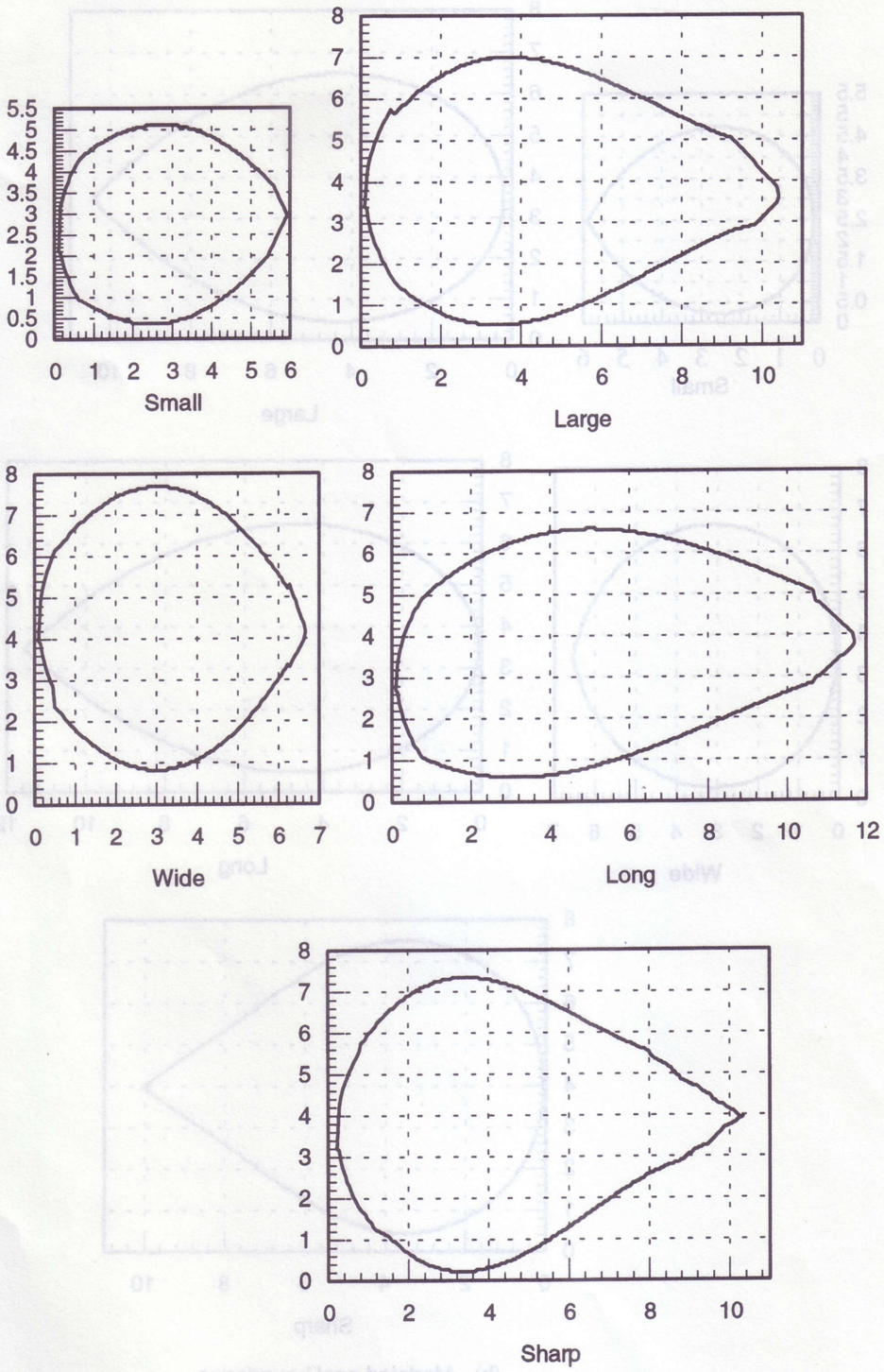

(a) - Original pool boundaries.

Fig. 10a. Modeling of different weld pools: original pool boundaries.

Figure 13 shows the neural network calculated parameters in the proposed polar coordinate model. Using these parameters, the weld penetration can also be calculated based on neural network. The results are shown in Fig. 14. It can be seen that the accuracy is very close to that acquired using the full description (length and nine relative widths). Thus, in addition to the geometry, the polar coordinate model also provides a satisfactory characterization of weld pool in specifying the weld penetration.

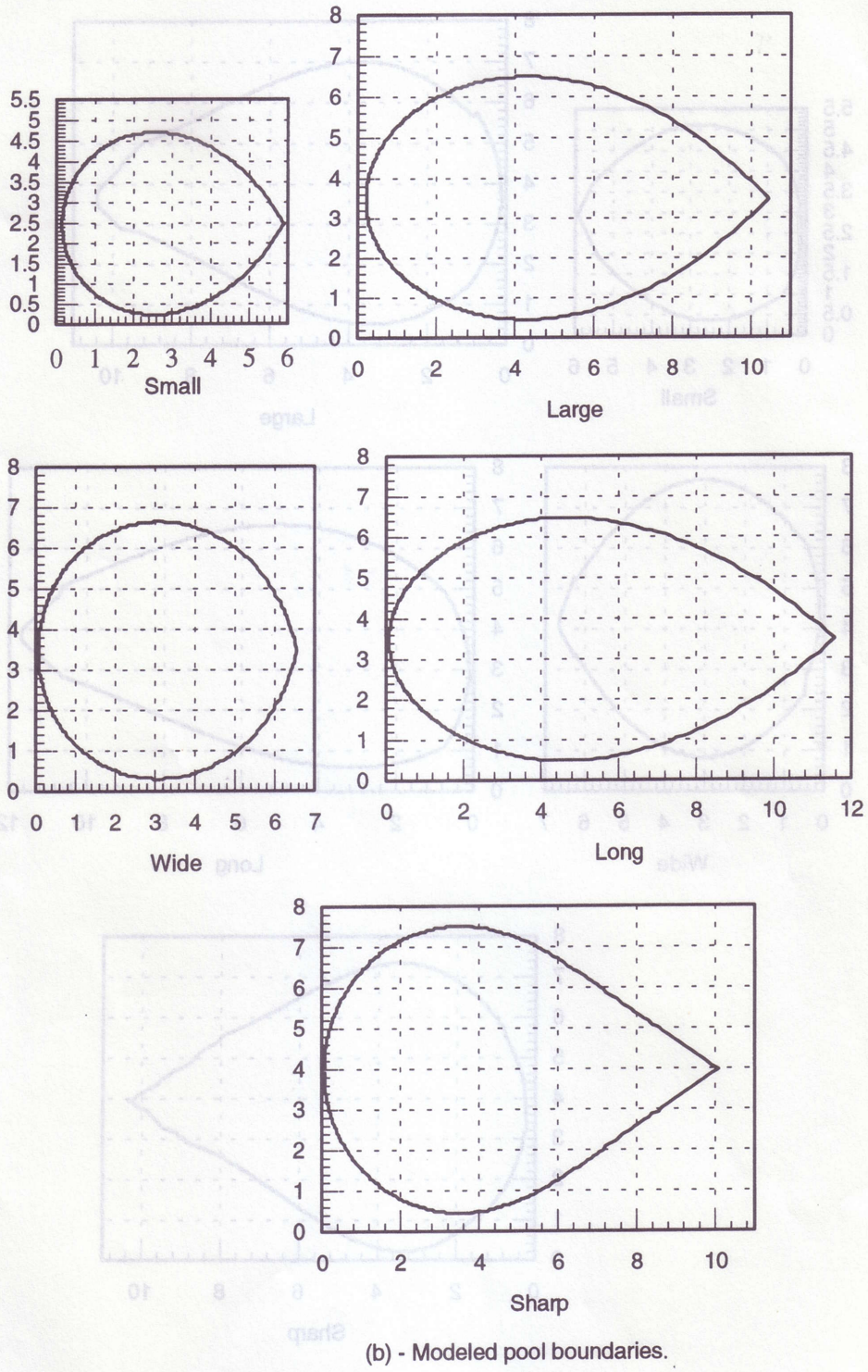

Fig. 10b. Modeling of different weld pools: modeled pool boundaries.

Model reduction

It is known that the weld pool shape is directly related to the grain structure in the weld [19]. Because the grain structure plays an important role in determining the mechanical properties of the joint, the desired pool shape should be achieved by closed-loop control. This control will be implemented by regulating the parameters in the proposed model. In the proposed polar coordinate model, four parameters are used. The weld pool

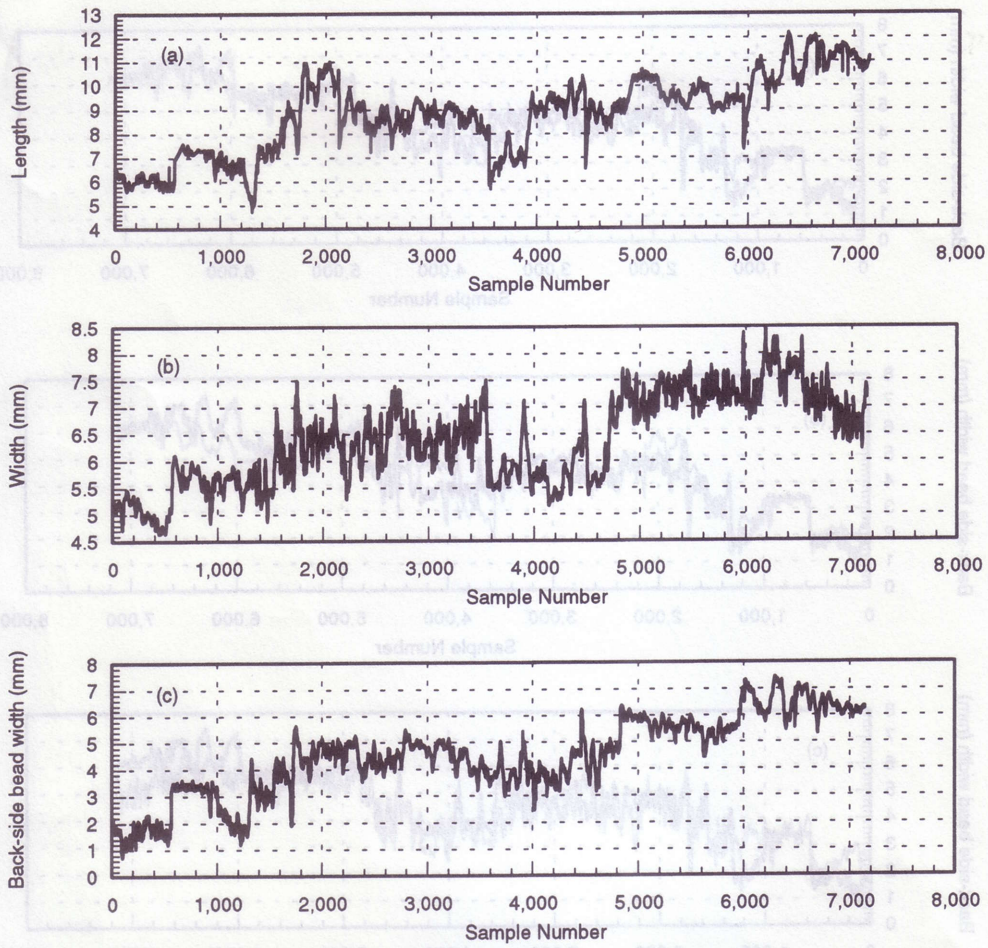

Fig. 11. Measured weld pool parameters: (a) length; (b) width; (c) back-side bead width. Experiment 1 from 1 to 566, experiment 2 from 567 to 1218, experiment 3 from 1219 to 2109, experiment 4 from 2110 to 3029, experiment 5 from 3030 to 3554, experiment 6 from 3555 to 4019, experiment 7 from 4020 to 4686, experiment 8 from 4687 to 5958, experiment 9 from 5959 to 7148.

can be sufficiently characterized. However, in order to control these four parameters, a very complicated control system will be required. Its implementation will be difficult.

In order to acquire a practical control system, the number of parameters in the polar coordinate model should be reduced. If both the pool geometry and weld penetration can be described with acceptable accuracy by the reduced model, a practical welding process control could be achieved.

It can be seen in Fig. 13(d) that θ_3 varies in a small range of about 6. In order to reduce the number of the parameters, θ_3 is replaced by 6. This replacement will produce an approximation error. However, because θ_2 is calculated using the constraint $\theta_1\pi^2 + \theta_2\pi^6 = L - 2\theta_0$, the approximation error can be partially compensated. Also, for practical control, trading-off may have to be considered. Thus we may propose the following reduced model:

$$r(\alpha) = \theta_0 + \theta_1\alpha^2 + \theta_2\alpha^6 \tag{9}$$

When the pool length L is known, only two θ_j's ($j = 0,1,2$) are independent. Thus, θ_j ($j = 0,1$) are selected as the outputs of the network, whereas θ_2 is calculated using the length constraint. The modeled weld pool boundaries obtained using the reduced model are shown in Fig. 15. For the grain structure control, the shapes acquired in Fig 15 can be regarded as sufficiently accurate. Figure 16 shows the weld penetration calculated based on the neural network by using the parameters in the reduced model. Its maximum error

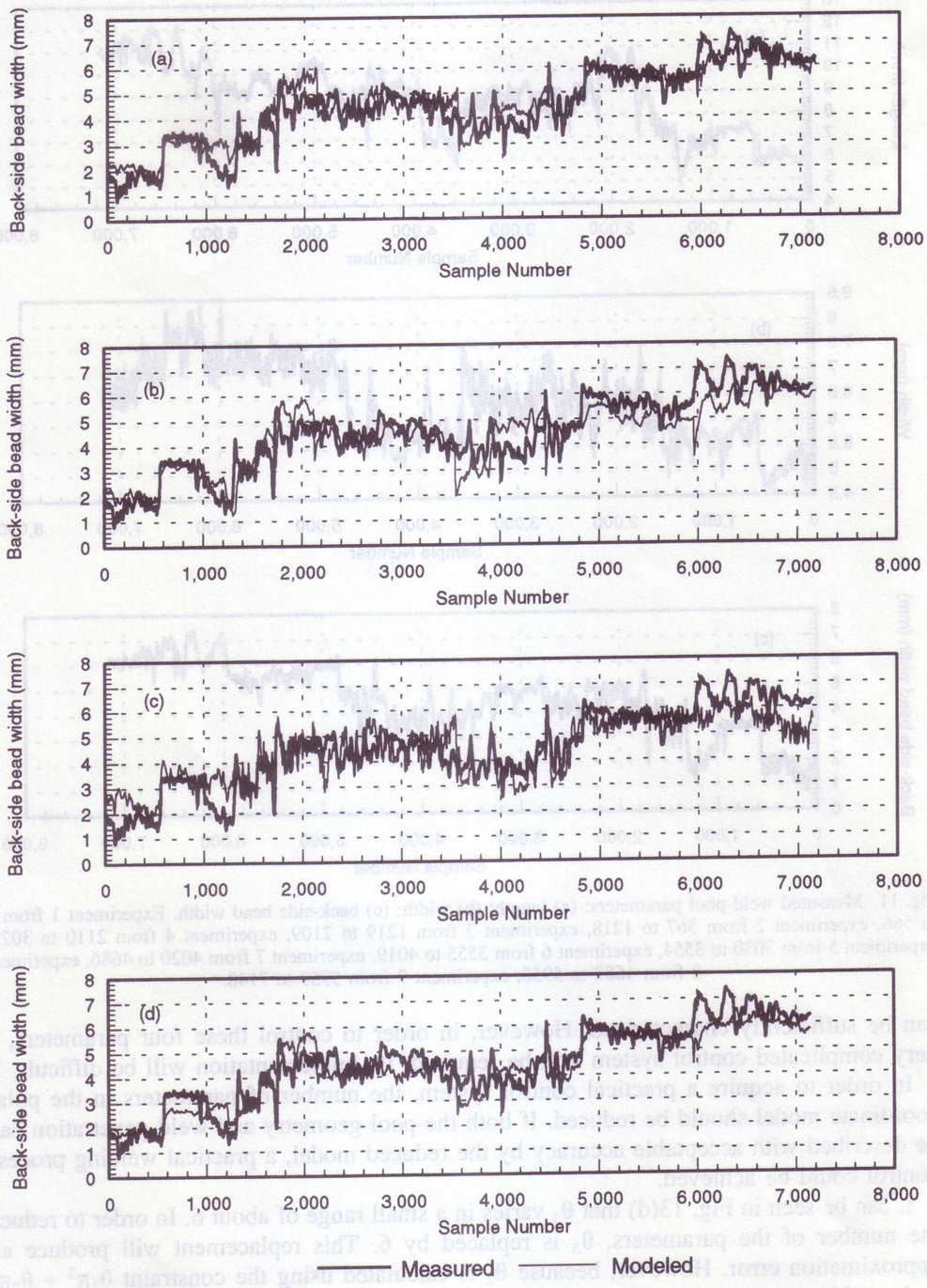

Fig. 12. Weld penetration modeling using weld pool parameters: (a) using nine relative widths and length; (b) using length; (c) using width; (d) using length and width.

in modeling the back side bead width is about 1 mm, which is again sufficient for the weld penetration control using a top-side sensor.

In order to identify most crucial parameters, each parameter in the reduced model can be used as an input for the neural network that calculates the weld penetration. Figure 17 shows the results. It can be seen that each individual parameter gives significant errors, whereas two parameters can provide much smaller errors. The maximum error when two parameters are used is about 1 mm. This is very close to the maximum error when three parameters are used (Fig. 14). Also, length and θ_0 (or θ_1) can generate better results than using θ_0 and θ_1. This implies that either the size parameter (length) or the shape parameter

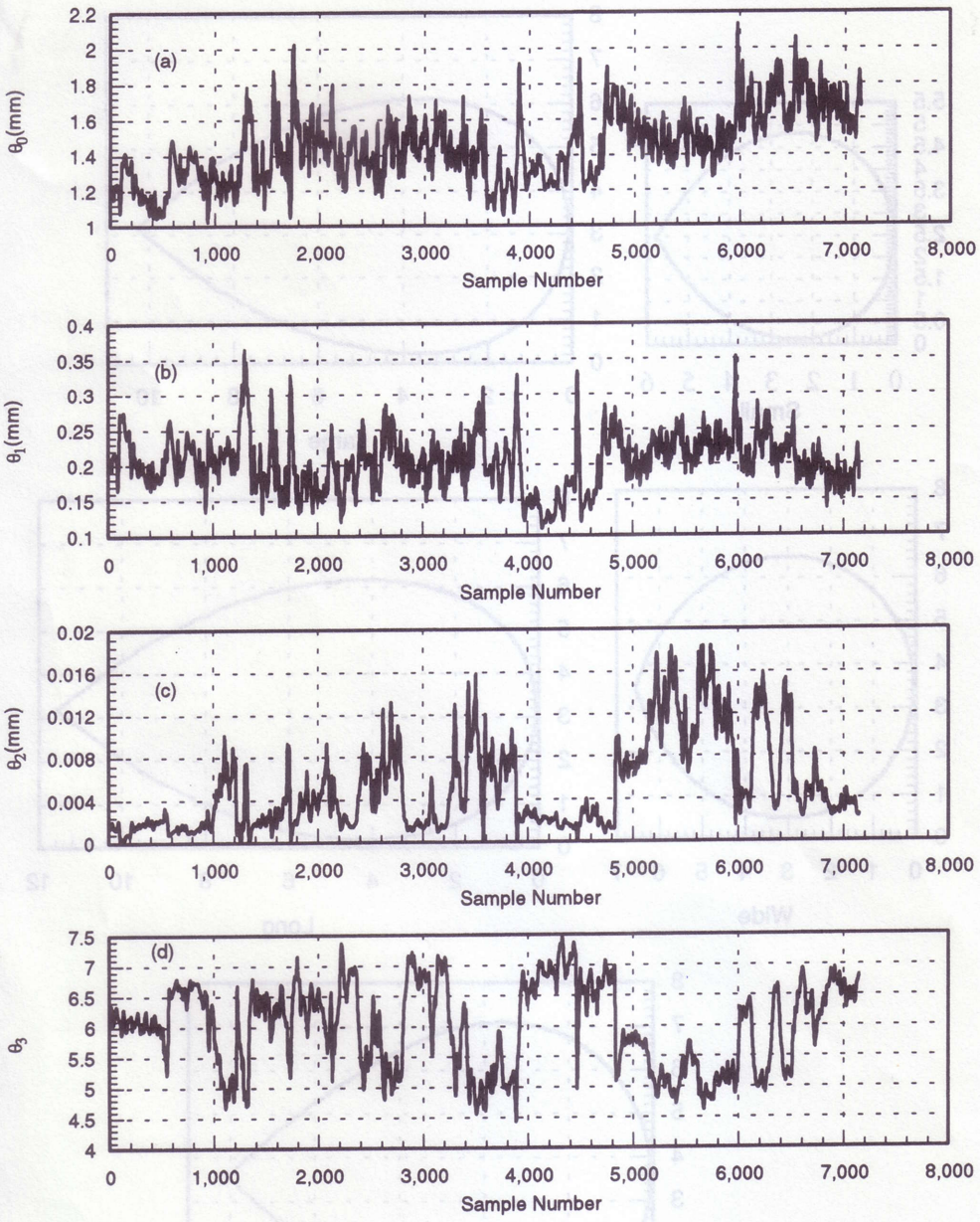

Fig. 13. On-line calculated parameters of the polar coordination model: (a) θ_0; (b) θ_1; (c) θ_2; (d) θ_3.

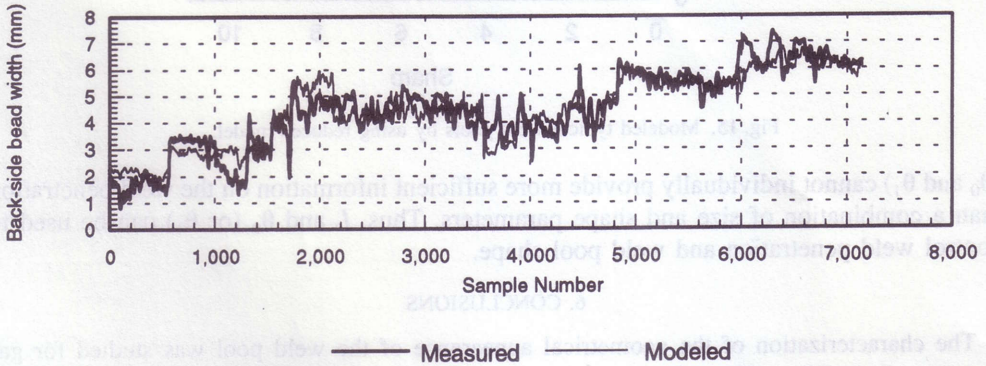

Fig. 14. Weld penetration modeling using the polar model parameters.

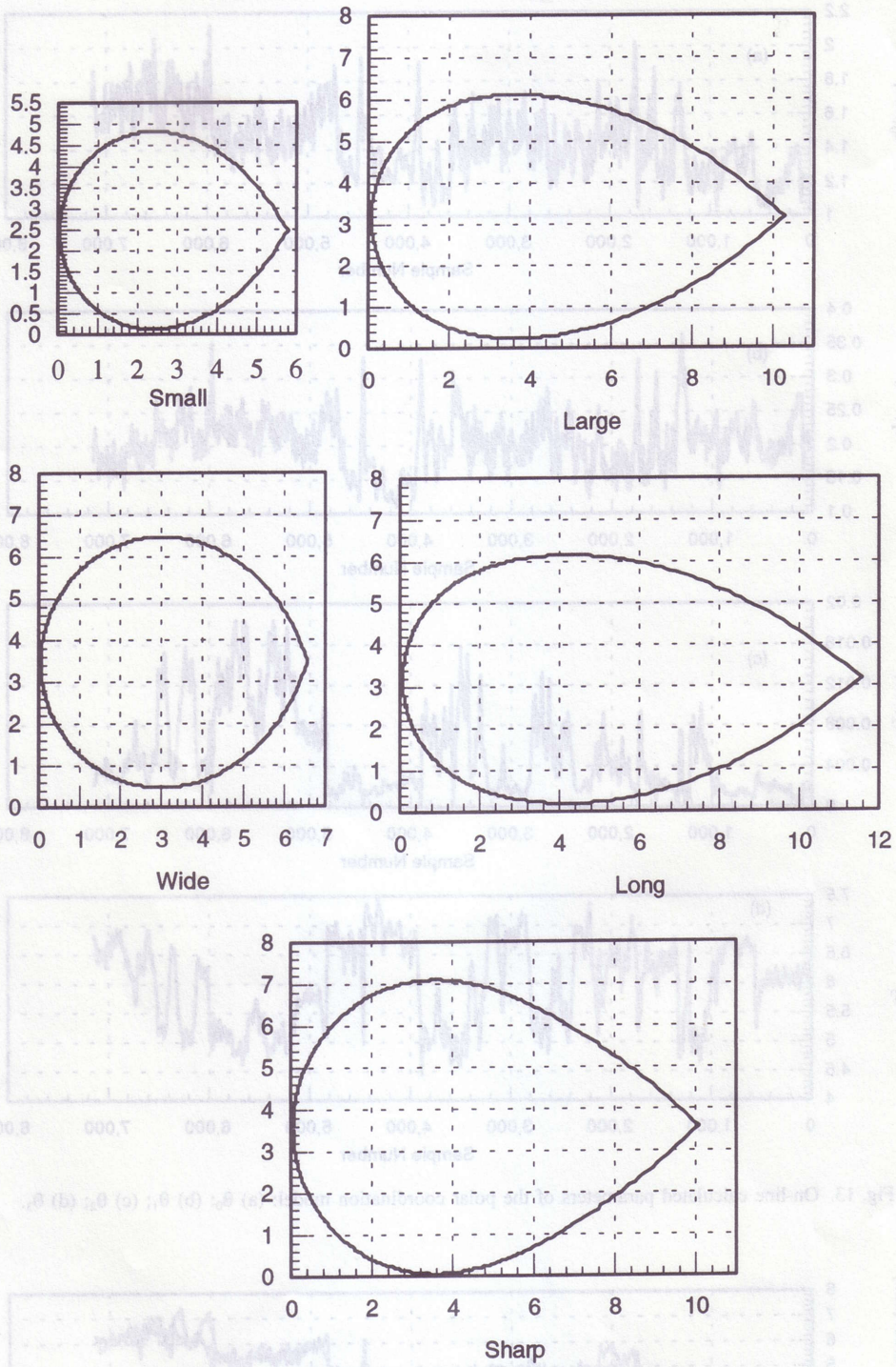

Fig. 15. Modeled typical weld pools by using reduced model.

(θ_0 and θ_1) cannot individually provide more sufficient information on the weld penetration than a combination of size and shape parameters. Thus, L and θ_0 (or θ_1) can be used to control weld penetration and weld pool shape.

6. CONCLUSIONS

The characterization of the geometrical appearance of the weld pool was studied for gas tungsten arc welding. The full penetration was addressed. The material was 3 mm stainless steel plates. The ranges of current, torch speed and arc length (see Table 1 and Fig. 3) were

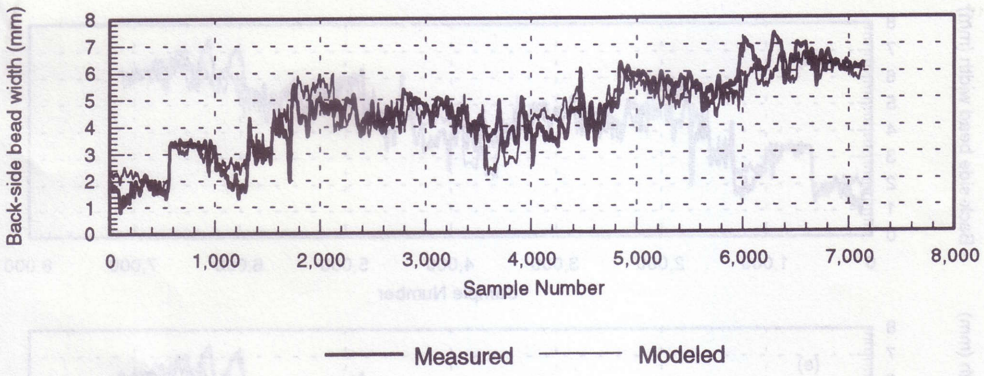

Fig. 16. Weld penetration modeling using the parameters of the parameter-reduced model.

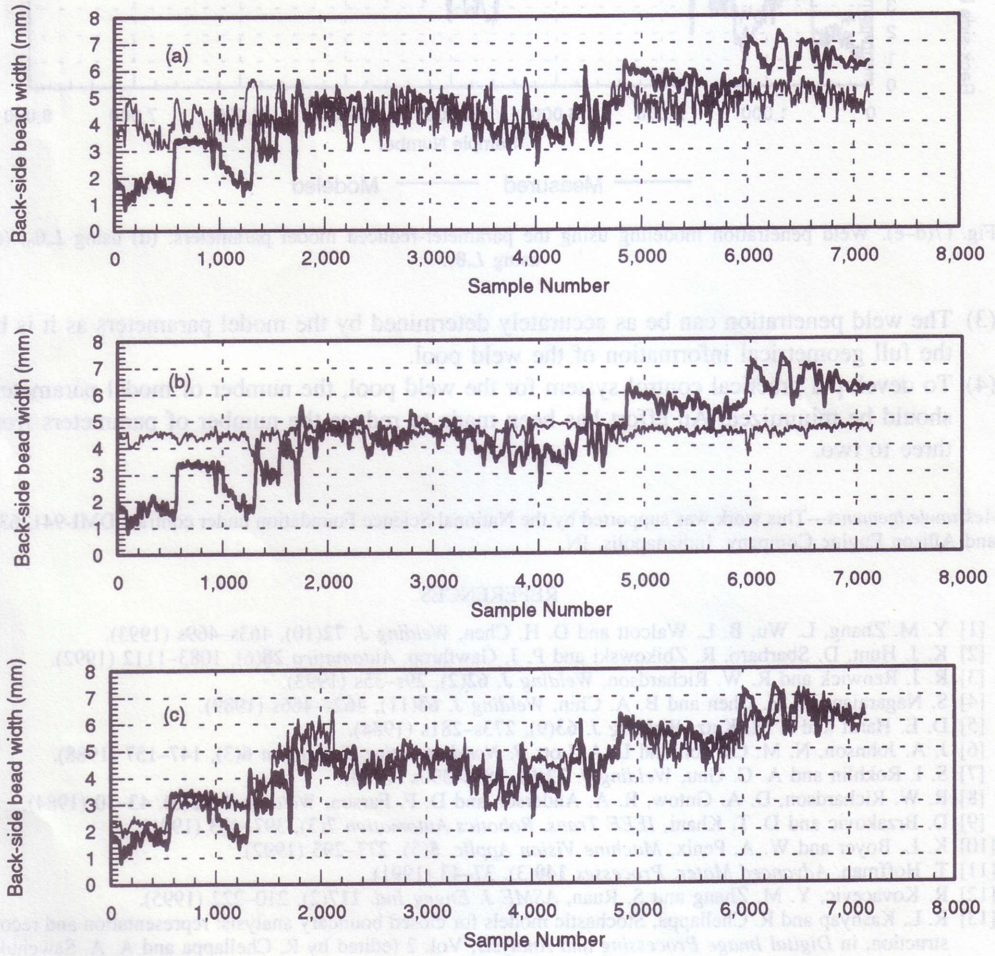

Fig. 17(a–c). Weld penetration modeling using the parameter-reduced model parameters: (a) using θ_0; (b) using θ_1; (c) using θ_0,θ_1.

selected to generate different fully penetrated weld pools. Based on these conditions, the following have been found:

(1) The geometrical appearance of the weld pool can be characterized by the proposed polar coordinate model. The parameters contained in the polar coordinate model correspond to different geometrical features of the weld pool.

(2) By the proposed neural network and the real-time image processing algorithm, the polar coordinate model parameters can be identified in real time.

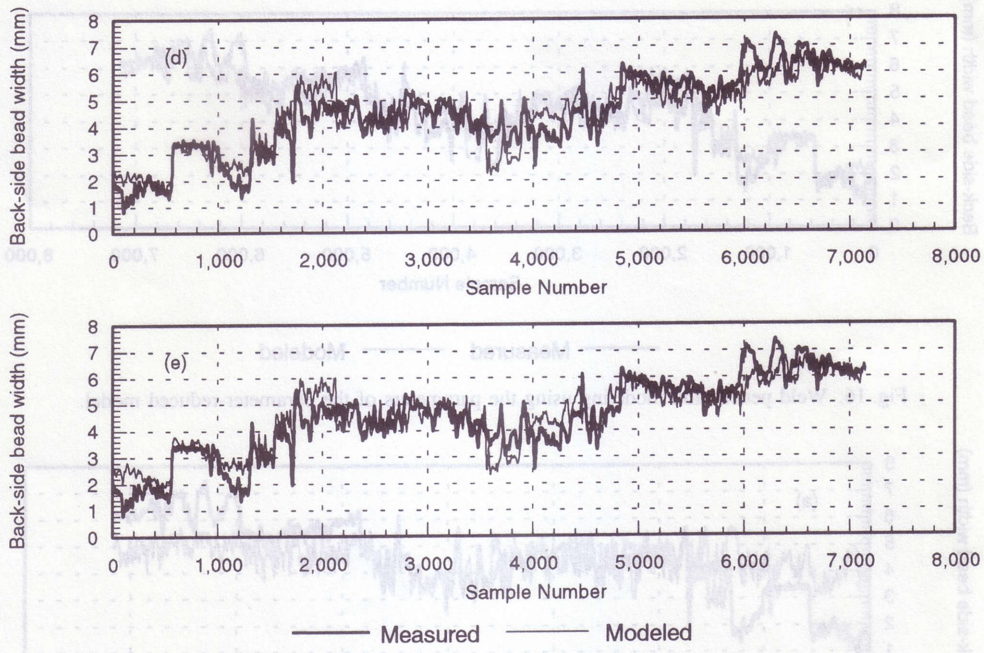

Fig. 17(d–e). Weld penetration modeling using the parameter-reduced model parameters: (d) using L,θ_0; (e) using L,θ_1.

(3) The weld penetration can be as accurately determined by the model parameters as it is by the full geometrical information of the weld pool.
(4) To develop a practical control system for the weld pool, the number of model parameters should be minimized. An effort has been made to reduce the number of parameters from three to two.

Acknowledgements—This work was supported by the National Science Foundation under contract DMI-9412637, and Allison Engine Company, Indianapolis, IN.

REFERENCES

[1] Y. M. Zhang, L. Wu, B. L. Walcott and D. H. Chen, *Welding J.* **72**(10), 463s–469s (1993).
[2] K. J. Hunt, D. Sbarbaro, R. Zbikowski and P. J. Gawthrop, *Automatica* **28**(6), 1083–1112 (1992).
[3] R. J. Renwick and R. W. Richardson, *Welding J.* **62**(2), 29s–35s (1993).
[4] S. Nagarajan, W. H. Chen and B. A. Chin, *Welding J.* **68**(11), 462s–466s (1989).
[5] D. E. Hardt and J. M. Katz, *Welding J.* **63**(9), 273s–281s (1984).
[6] J. A. Johnson, N. M. Carlson and L. A. Lott, *J. Nondestructive Evaluation* **6**(3), 147–157 (1988).
[7] S. I. Rokhlin and A. C. Guu, *Welding J.* **72**(8), 381s–390s (1993).
[8] R. W. Richardson, D. A. Gutow, R. A. Anderson and D. F. Farson, *Welding J.* **63**(3), 43–50 (1984).
[9] D. Brzakovic and D. T. Khani, *IEEE Trans. Robotics Automation* **7**(3), 397–403 (1991).
[10] K. L. Boyer and W. A. Penix, *Machine Vision Applic.* **5**(5), 277–293 (1992).
[11] T. Hoffman, *Advanced Mater. Processes* **140**(3), 37–43 (1991).
[12] R. Kovacevic, Y. M. Zhang and S. Ruan, *ASME J. Engng Ind.* **117**(2), 210–222 (1995).
[13] R. L. Kashyap and R. Chellappa, Stochastic models for closed boundary analysis: representation and reconstruction, in *Digital Image Processing and Analysis*, Vol. 2 (edited by R. Chellappa and A. A. Sawchuk), pp. 109–119. IEEE Computer Society (1985).
[14] S. M. Pandit and W. M. Wu, *Time Series and System Analysis with Applications*, Chap. 2. John Wiley, New York (1983).
[15] *Using NeuralWorks: Professional II/Plus and NeuralWorks Explorer*. NeuralWare Inc., Pittsburgh, PA (1993).
[16] Y. M. Zhang, R. Kovacevic and L. Wu, *ASME J. Engng Ind.* **118**(1), 123–136 (1996).
[17] Y. H. Xiao and G. den Ouden, *Welding J.* **72**(8), 428s–434s (1993).
[18] W. Chen and B. A. Chin, *Welding J.* **69**(4), 181s–185s (1990).
[19] S. Kou and Y. Le, *Metal. Trans.* **19A**, 1075–1082 (1988).